Eur Respir J 2012; 39: 546–557
DOI: 10.1183/09031936.00047111

NiO and Co_3O_4 nanoparticles induce lung DTH-like responses and alveolar lipoproteinosis

W-S. Cho*,#, R. Duffin*, M. Bradley¶, I.L. Megson+, W. MacNee*, S.E.M. Howie§ and K. Donaldson*

ABSTRACT: Lung exposure to metal oxide nanoparticles (NPs) comprising soluble metal haptens may produce T-helper cell type 1 (Th1)- and Th17-associated delayed-type hypersensitivity (DTH) responses and pulmonary alveolar proteinosis (PAP).

In order to study this, haptenic metal oxide NPs (NiO, Co_3O_4, Cr_2O_3 and CuO) were instilled into the lungs of female Wistar rats, and the immunoinflammatory responses were assessed at 24 h and 4 weeks post-instillation. Primary culture of alveolar macrophages from Wistar rats was used to evaluate the effect of the NPs on the ability to clear surfactant.

NiO NPs induced chronic interstitial inflammation and pro-inflammatory Th1 and Th17 immune responses characterised by increases in the cytokines monocyte chemotactic protein (MCP)-1/CCL2, interleukin (IL)-12 p40, interferon-γ and IL-17A, whilst similar pathological responses induced by Co_3O_4 NPs were associated with increases in MCP-1/CCL2 and IL-12 p40. However, neither Cr_2O_3 nor CuO NPs elicited immunoinflammatory reactions. PAP was induced by both NiO and Co_3O_4 NPs during the chronic phase. PAP was associated with over-production of surfactant by proliferation of type II cells and impaired clearance of surfactant by macrophages.

These findings have implications for the risk management of occupational NP exposure and provide evidence that haptenic metal oxide NPs can induce chronic progressive lung immune responses *via* a DTH-like mechanism.

KEYWORDS: Delayed-type hypersensitivity, hapten, metal oxide nanoparticles, pulmonary alveolar proteinosis, rat

Metal oxide nanoparticles (NPs) are known to release metal ions that can contribute to their toxicity [1, 2]. Some metal ions are known to induce contact dermatitis *via* delayed-type hypersensitivity (DTH) mediated by a cluster of differentiation (CD)4 T-cell-dependent inflammatory immune response that involve T-helper type 1 (Th1) and/or Th17 effector CD4 T-cells [3–5]. Those metal ions triggering immune responses may be regarded as haptens, low molecular weight species that are not themselves antigenic, but when bound to a host protein elicit sufficient structural change in the protein and its processed peptides that they can be recognised as nonself by T-cells [6]. This may lead to the development of autoimmunity [7]. Metal haptens include nickel, cobalt, chromium and copper, and 10–15% of the general population shows an allergic response to at least one of these metal ions [8]. The use of medical metal implants leading to raised levels of metal ions in serum has raised concern about metal hypersensitivity or carcinogenicity in patients [9].

Currently, large-scale production of metal oxide NPs for industrial, cosmetic and medical imaging purposes raises the likelihood of inhalation exposure in occupational, consumer and clinical settings. Although metal haptens can cause DTH in the skin, it is not known whether, following deposition in the lungs, NPs containing haptenic metals can induce similar immunoinflammatory effects there. Other human lung pathologies associated with inhalation of particles include pulmonary alveolar proteinosis (PAP), which is characterised by an accumulation of surfactant proteins and lipids in the alveoli [10, 11]. Our previous study with NiO NPs was the first to report induction of PAP by NP exposure [12]. PAP in

AFFILIATIONS
*ELEGI/Colt Laboratory, Centre for Inflammation Research, University of Edinburgh,
§Immunology Group, Centre for Inflammation Research, University of Edinburgh,
¶School of Chemistry, University of Edinburgh, Edinburgh,
+Free Radical Research Facility, UHI Dept of Diabetes and Cardiovascular Science, Centre for Health Science, Inverness, UK.
#Dept of Medicinal Biotechnology, College of Natural Resources and Life Sciences, Dong-A University, Busan, South Korea.

CORRESPONDENCE
K. Donaldson
Queens Medical Research Institute
University of Edinburgh
47 Little France Crescent
Edinburgh EH16 4TJ
UK
E-mail: ken.donaldson@ed.ac.uk

Received:
March 16 2011
Accepted after revision:
July 11 2011
First published online:
Aug 04 2011

European Respiratory Journal
Print ISSN 0903-1936
Online ISSN 1399-3003

This article has supplementary material available from www.erj.ersjournals.com

humans can also be caused by an autoimmune response to granulocyte macrophage colony-stimulating factor (GM-CSF) [13]. However, whether other haptenic metal NPs can cause PAP and by which underlying mechanisms is not known.

In our previous study, we tested a number of different NPs for lung toxicity and found that they induced unique inflammatory footprints, including neutrophilic, eosinophilic and mononuclear inflammation [12]. In particular, we found that NPs containing the metal hapten NiO induced lymphocytic inflammation and PAP at 4 weeks after instillation into rat lungs. Here, a panel of NPs was assembled comprising the oxides of haptenic metals (NiO, Co_3O_4, Cr_2O_3 and CuO) and these were instilled into the lungs of rats. Their immunoinflammatory potential and propensity to produce PAP were then evaluated and the underlying mechanisms were examined.

MATERIALS AND METHODS

NPs and characterisation

Metal oxide NPs were purchased from commercial sources: NiO and Co_3O_4 NPs from Nanostructural and Amorphous Materials Inc. (Houston, TX, USA); Cr_2O_3 NPs from IOLITEC (Heilbronn, Germany); and CuO NPs from Sigma-Aldrich (Poole, UK). The primary size and shape of the NPs was measured by transmission electron microscopy (TEM) (JEM-1200EX II; JEOL, Tokyo, Japan). The surface areas of the NPs were determined by BET (Brunauer–Emmett–Teller) analysis using a Micromeritics TriStar 3000 (Micromeritics UK Ltd, Dunstable, UK). NPs were dispersed in saline with 5% heat-inactivated rat serum as previously described [12]. Briefly, the stock concentration of NPs was dispersed with distilled water at 6,000 $cm^2 \cdot mL^{-1}$ and sonicated using a probe sonicator (Philip Harris Scientific, Lichfield, UK) for 30 s at 50% power. The NP stock (final concentration 300 $cm^2 \cdot mL^{-1}$) and heat-inactivated rat serum (final concentration 5%) were mixed prior to addition of 0.9% physiological saline. The zeta potential of NPs, a measurement of surface charge, was checked using a Zetasizer-Nano ZS (Malvern Instruments Ltd, Malvern, UK), and hydrodynamic size and polydispersity in suspensions was analysed using a Brookhaven 90 Plus (Brookhaven Instruments Corp., Holtsville, NY, USA). The levels of lipopolysaccharide contamination in the NP suspensions were evaluated by a *Limulus* amoebocyte lysate assay (Cambrex, Walkersville, MD, USA).

Solubility test of NPs

To evaluate the solubility of NPs in conditions mimicking the lung environment, NPs at 300 $cm^2 \cdot mL^{-1}$ were incubated with artificial lysosomal fluid (pH 5.5) or artificial interstitial fluid (pH 7.4) for 24 h and 4 weeks. Artificial lysosomal fluid and artificial interstitial fluid were prepared as described previously [14, 15]. After each time-point, the dissolved ions were collected by three rounds of centrifugation (15,000 × *g* for 20 min) and measured by inductively coupled plasma–atomic emission spectrometry (Optima 5300 DV; PerkinElmer, Cambridge, UK). As a control, NPs dispersed in saline at 300 $cm^2 \cdot mL^{-1}$ were incubated for 24 h and water-soluble metal ions of the supernatant collected as described were measured using inductively coupled plasma–mass spectrometry (Agilent 7500ce; Agilent Technologies, Stockport, UK).

Animal experiment

NPs were dispersed in saline with 5% rat serum for intratracheal instillation into rats. 6-week-old female Wistar rats (200–250 g) were purchased from a specific pathogen-free colony at Harlan Laboratories (Hillcrest, UK) and quarantined for 7 days prior to commencement of the study. Water and a normal diet were available *ad libitum*. The rats were maintained and handled under a specific licence granted by the Home Office (London, UK) that ensures humane treatment and alleviation of suffering in all animal experiments. Rats were randomly assigned to groups based on body weight and NPs were instilled at the same surface area dose. In our previous studies, we tested several NP types at surface area doses of 50, 150 and 250 cm^2 per rat, and 150 cm^2 per rat showed a clear discrimination among NP types [1, 12]. Therefore, we chose the surface area for instillation as 150 cm^2 per rat, and the equivalent mass doses for NiO, Co_3O_4, Cr_2O_3 and CuO NPs were 163.5, 419.0, 201.6 and 515.0 μg, respectively. 10 rats were used as a vehicle control (5% rat serum in saline), while five rats were used for the other groups. When experiments were repeated, vehicle controls were always included and so the number built up, eventually reaching 10 rats. Rats were anaesthetised using isoflurane and the trachea was cannulated with a laryngoscope. 500 μL of the suspensions of NPs were instilled into the lungs and the rats were sacrificed at 24 h or 4 weeks post-instillation. At each time-point, rats were sacrificed by peritoneal injection of sodium pentobarbitone (200 mg per rat) and blood was taken from the caudal vena cava. Bronchoalveolar lavage (BAL) was obtained by cannulating the trachea with a luer port cannula (Portex, Ashford, UK) connected to a syringe and the lungs were lavaged four times with 8 mL of saline. The first lavage was kept for total protein, lactate dehydrogenase and cytokine measurements. All four lavages were pooled for cytological analysis.

Preparation of BAL

Cytospin slides of the BAL were prepared as previously described [12]. Briefly, BAL was centrifuged at 250 × *g* for 5 min and resuspended in 1 mL PBS. The total number of cells was counted using a nucleocounter (Chemometec, Allerød, Denmark) and 10,000 cells were attached to glass slides by cytospin at 15 × *g* for 5 min. The slides were fixed with 100% methanol and stained with Diff-Quik (Raymond Lamb, Eastbourne, UK). In each sample, more than 500 cells were counted for differential cell counts according to their morphological characteristics using a light microscope.

Measurement of phospholipids and total proteins in the BAL

The concentration of phospholipids in the BAL was measured using a phospholipids assay kit (Bioassay Systems, Hayward, CA, USA). Levels of total proteins in the BAL were measured using a bicinchoninic acid assay (Sigma-Aldrich).

ELISA for inflammatory mediators

To evaluate the immunological responses, GM-CSF, monocyte chemotactic protein (MCP)-1/ CCL2, macrophage inflammatory protein (MIP)-2/CXCL2, interleukin (IL)-12 p40, and Th1 (interferon (IFN)-γ), Th2 (IL-4) and Th17 (IL-17A) cytokines were measured using commercially available ELISA kits (MCP-1/CCL2: BD, Oxford, UK; IL-12 p40: Invitrogen, Paisley, UK; IL-17A: eBioscience, Hatfield, UK; GM-CSF, MIP-2/CXCL2, IFN-γ and IL-4: R&D Systems, Minneapolis, MN, USA). Cytokines in serum (1:2 dilution) and BAL (undiluted) samples were measured according to the manufacturer's instructions.

Measurement of autoantibodies for GM-CSF in the serum and BAL

To measure the levels of the autoantibodies to GM-CSF, the rat GM-CSF Duoset kit from R&D Systems was used. Instead of the capture antibody, serum (1:2–1:200 dilution) or undiluted BAL fluids were used to coat 96-well plates. After blocking with 1% bovine serum albumin in PBS, GM-CSF standard (250 pg·mL^{-1}) was applied to the serum- or BAL-coated wells for 2 h. Detection antibody, streptavidin–horseradish peroxidase, substrate (tetramethylbenzidine) and stop solution were sequentially applied as indicated in the instruction manual.

Immunohistochemistry for CD3, CD45RA and Ki-67

To evaluate the cell types infiltrated into the BAL, we performed immunohistochemistry for CD3, which is specific for mature T-cells, and CD45RA, which is specific for B-cells, natural killer cells and naïve T-cells. Cytospin slides were hydrated in distilled water and hydrogen peroxide (3%) was applied for 15 min to quench the activity of endogenous peroxidase. Slides were blocked with normal goat serum and anti-rat CD3 antibody (AbD Serotec, Oxford, UK) or anti-rat CD45RA antibody (AbD Serotec) was applied at a 1:100 dilution. Slides were washed three times and incubated for 30 min at room temperature with the Envison anti-mouse IgG kit (Dako, Ely, UK). The slides were then washed a further three times and 3,3′-diaminobenzidine (DAB) substrate (Vector Laboratories, Peterborough, UK) was applied.

To evaluate the cellular proliferation, Ki-67 immunohistochemistry was performed on paraffin-embedded sections of lung tissues. Briefly, 3-μm paraffin lung sections were dewaxed and hydrated using a xylene–alcohol series. Endogenous peroxidase activity was quenched by incubating with hydrogen peroxide (3%) at room temperature for 15 min. Antigen retrieval was performed by incubating with Borg Decloaker (Biocare Medical, Concord, CA, USA) for 2 min. Anti-human Ki-67 antibody (Abcam, Cambridge, UK) was applied at a 1:50 dilution. Envision anti-mouse IgG kit and DAB substrate were applied sequentially. Ki-67-positive cells in the alveolar epithelium were counted. More than 4,000 cell nuclei were counted in the alveolar epithelial cells in alveoli, excluding blood vessels and bronchioles, by microscopy at 400× magnification. Percentages of Ki-67-positive cells were determined on four slides in each group and expressed as mean±SD.

Histological analysis

One nonlavaged and four post-lavaged lungs were inflated with 10% neutral-buffered formalin and fixed overnight. Lungs were then trimmed, processed and waxed using routine histological processes. Paraffin blocks were cut into 3-μm sections and stained with haematoxylin and eosin. Routine periodic acid–Schiff (PAS) staining was used to measure glycoprotein accumulation. The number of lymphocyte aggregates in the alveoli, excluding peribronchial lymph nodes, in each lung section of all lobes was counted and multiplied by a factor representing the diameter of aggregates as follows: 1, <50 μm; 2, 50–200 μm; and 3, >200 μm.

Transmission electron microscopy

To evaluate the ultrastructural pulmonary changes induced by haptenic NPs, we selected NiO NPs as a representative NP inducing DTH and PAP, and instilled at 150 cm^2. After 4 weeks, lungs of vehicle control and NiO NP treatment were fixed with 1.5% glutaraldehyde in 0.1 M cacodylate buffer. The lung tissues were then stained *en bloc* with uranyl acetate and embedded in epoxy resin. Ultrathin (60-nm) sections were cut, stained with uranyl acetate and lead citrate, and examined by TEM.

Test of alveolar macrophage function on clearance of dipalmitoylphosphatidylcholine

Surfactant is composed of ~90% lipids and ~10% proteins [16]. Phospholipids and phosphatidylcholine comprise 80–90% of the lipids. Dipalmitoylphosphatidylcholine (DPPC) is the major component (60%) of phosphatidylcholine. The physiological levels of surfactant lipids within the lung have been estimated to be 100–500 μg·mL^{-1} [17]. To evaluate the effects of particle overload on the clearance of DPPC, we extracted alveolar macrophages from Wistar rats prior to culture in 24-well plates (Nunc, Roskilde, Denmark) at a density of 1×10^6 cells·mL^{-1}. RPMI medium (PAA Laboratories, Somerset, UK) containing 10% fetal bovine serum, 2 mM L-glutamine (Life Technologies,

TABLE 1 Physicochemical analysis of metal oxide nanoparticles

Measurement	NiO	Co_3O_4	Cr_2O_3	CuO
Primary size[#] nm	5.3±1.9	18.4±5.0	205±129	23.1±7.2
Hydrodynamic size[¶] nm	92.50±4.10	185.2±31.3	136.2±60.2	112.1±17.3
Polydispersity[¶]	0.21±0.07	0.10±0.02	0.68±0.04	0.19±0.01
Surface area[+] $m^2 \cdot g^{-1}$	91.8	35.8	74.42	29
Zeta potential[§] mV	-21.0±5.0	-21.6±0.7	-28.3±6.0	-25.3±4.4
Endotoxin[ƒ]	ND	ND	ND	ND
Mass per animal μg	163.5	419.0	201.6	515.0
Metal ions[##,¶¶] ppm	**Ni(II)**	**Co(II, III)**	**Cr(III)**	**Cu(II)**
24 h				
Saline	4.00 (1.56)	0.09 (0.02)	1.70 (0.62)	5.00 (0.61)
Basic	3.97 (1.16)	0.08 (0.01)	4.34 (1.58)	5.38 (0.65)
Acid	22.9 (8.93)	9.74 (1.58)	4.05 (1.47)	804 (97.3)
4 weeks				
Basic	6.47 (2.52)	0.07 (0.01)	0.00 (0.00)	7.98 (0.97)
Acid	87.6 (34.1)	51.3 (8.34)	3.50 (1.27)	832 (100)

Data are presented as mean±SD, unless otherwise stated. ND: not detected. [#]: measured by transmission electron microscopy; [¶]: of nanoparticles (NPs) dispersed with 5% rat serum in saline was determined using a Brookhaven 90 Plus (Brookhaven Instruments Corp., Holtsville, NY, USA); [+]: measured with a Micromeritics TriStar 3000 (Micromeritics UK Ltd, Dunstable, UK); [§]: of NPs dispersed with 5% rat serum in saline was measured using a Zetasizer-Nano ZS (Malvern Instruments Ltd, Malvern, UK); [ƒ]: measured by a *Limulus* amoebocyte lysate assay (Cambrex, Walkersville, MD, USA) and the detection limit was 10 pg·mL^{-1}; [##]: water-soluble metal ions of NPs in saline, artificial interstitial fluid (basic, pH 7.4) or artificial lysosomal fluid (acid, pH 5.5) were analysed by inductively coupled plasma–mass spectrometry (Agilent 7500ce; Agilent Technologies, Stockport, UK) or inductively coupled plasma–atomic emission spectrometry (Optima 5300 DV; PerkinElmer, Cambridge, UK); [¶¶]: data in parentheses represent the percentage of dissolution compared with the initial mass.

Paisley, UK), 100 IU·mL^{-1} penicillin and 100 U·mL^{-1} streptomycin (Life Technologies) was used. After 2 h incubation, cells were washed with pre-warmed PBS, and treated with NPs at 30 and 100 cm^2·mL^{-1} for NiO, Co_3O_4 and Cr_2O_3 NPs, or 3 and 10 cm^2·mL^{-1} for CuO NPs for 2 h. The different dose scheme between CuO and other NPs was selected based on cytotoxicity; CuO NP showed ~10-fold higher cytotoxicity than other NPs. Then, NPs were washed with pre-warmed PBS and synthetic DPPC (L-α-phosphatidylcholine dipalmitoyl; Sigma-Aldrich) was applied at 250 μg·mL^{-1} for a further 22 h. The turbidity of the supernatant was measured as the absorbance at 600 nm. Absorbances of DPPC-treated groups were corrected by subtracting those of fresh medium and quantified by plotting a standard curve. The levels of phospholipids were measured in the serially diluted DPPC and supernatant according to the manufacturer's instructions (Bioassay Systems). Cells were also collected by brief pipetting and cytospins were prepared as described above.

Instillation of NiO NPs without dispersion medium

To evaluate the effects of serum coating on the surface of NPs, NiO NPs were selected as an exemplar NP because they showed the most severe toxicity in our panel of NPs. The same surface area dose of NiO NPs without dispersion medium, and therefore having large aggregates (hydrodynamic size 6,393±1,028 nm), was instilled into the lungs of rats that were sacrificed 4 weeks after instillation. BAL fluid analysis, and measurement of phospholipids and total protein in the BAL were performed using the aforementioned methods. Four rats were used for instillation and the data were compared with the vehicle control and well-dispersed NiO NPs.

Statistical analysis

Data were analysed with GraphPad InStat Software (version 5; GraphPad Software Inc., La Jolla, CA, USA). Data are presented as mean±SD. To compare each treatment group, one-way ANOVA with *post hoc* Tukey's pairwise comparisons was applied. A p-value <0.05 was considered to be statistically significant.

RESULTS

Physicochemical analysis of NPs

Table 1 summarises the size, surface area, hydrodynamic size, polydispersity, zeta potential and endotoxin level of the NP panel. The size distribution measured by TEM showed that NiO, Co_3O_4 and CuO NPs had a narrow size distribution consistent with the measure of polydispersity, while Cr_2O_3 NPs showed a more heterogeneous size distribution (table 1 and online supplementary fig. S1). All NPs were well dispersed and showed negative zeta potentials, with no endotoxin found.

Solubility of NPs under acid and basic conditions

All NPs showed minimal dissolution in physiological saline and artificial interstitial fluid (pH 7.4), while solubility of NPs in the artificial lysosomal fluid (pH 5.5) was heterogeneous, with solubility in the order CuO>NiO>Co_3O_4>Cr_2O_3 (table 1 and online supplementary fig. S2). It was notable that CuO

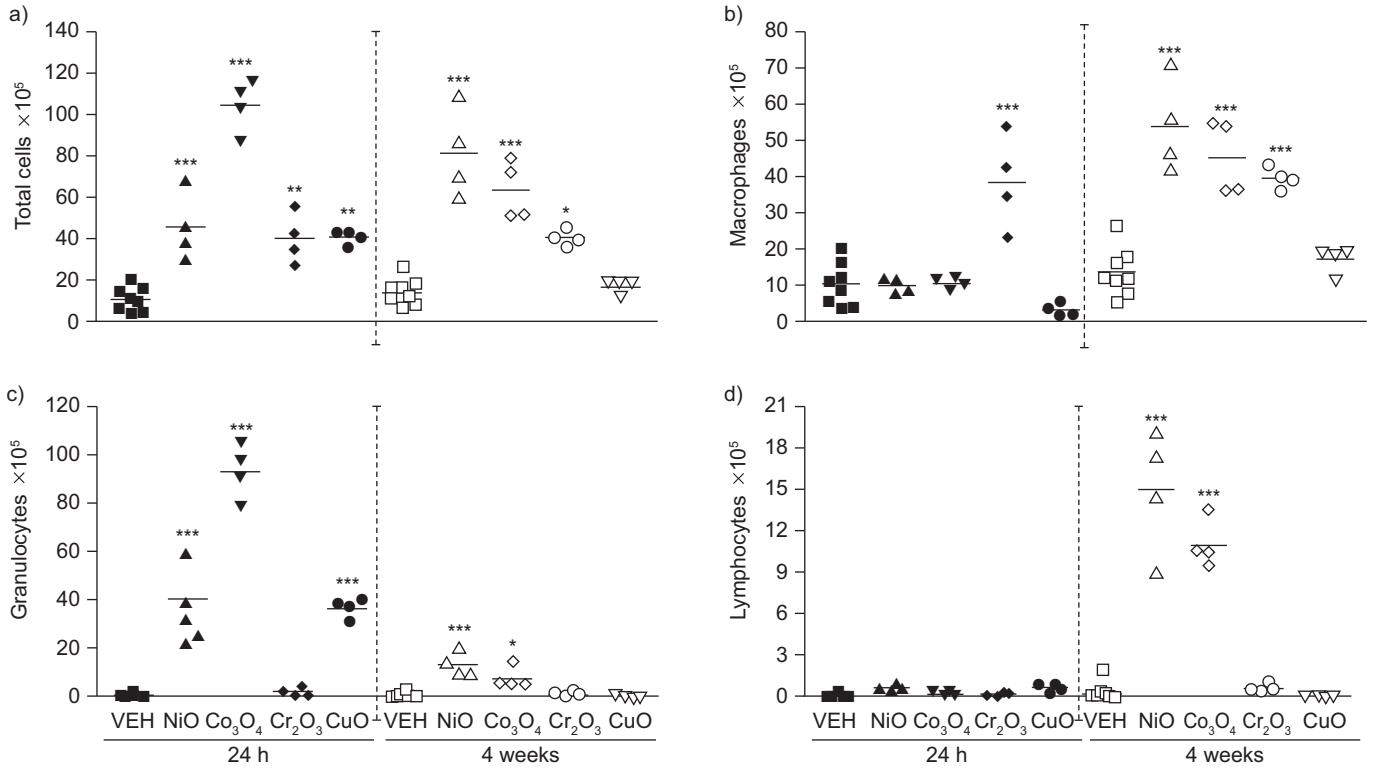

FIGURE 1. Differential cell counts of bronchoalveolar lavage fluid at 24 h or 4 weeks after instillation of metal oxide nanoparticles at 150 cm^2. a) Total number of cells; b) number of macrophages; c) total number of granulocytes; d) number of lymphocytes. n=8 for all vehicle control and n=4 for other treatment groups. —: mean. Each treatment group was compared with vehicle control (VEH) for statistical significance. *: p<0.05; **: p<0.01; ***: p<0.001.

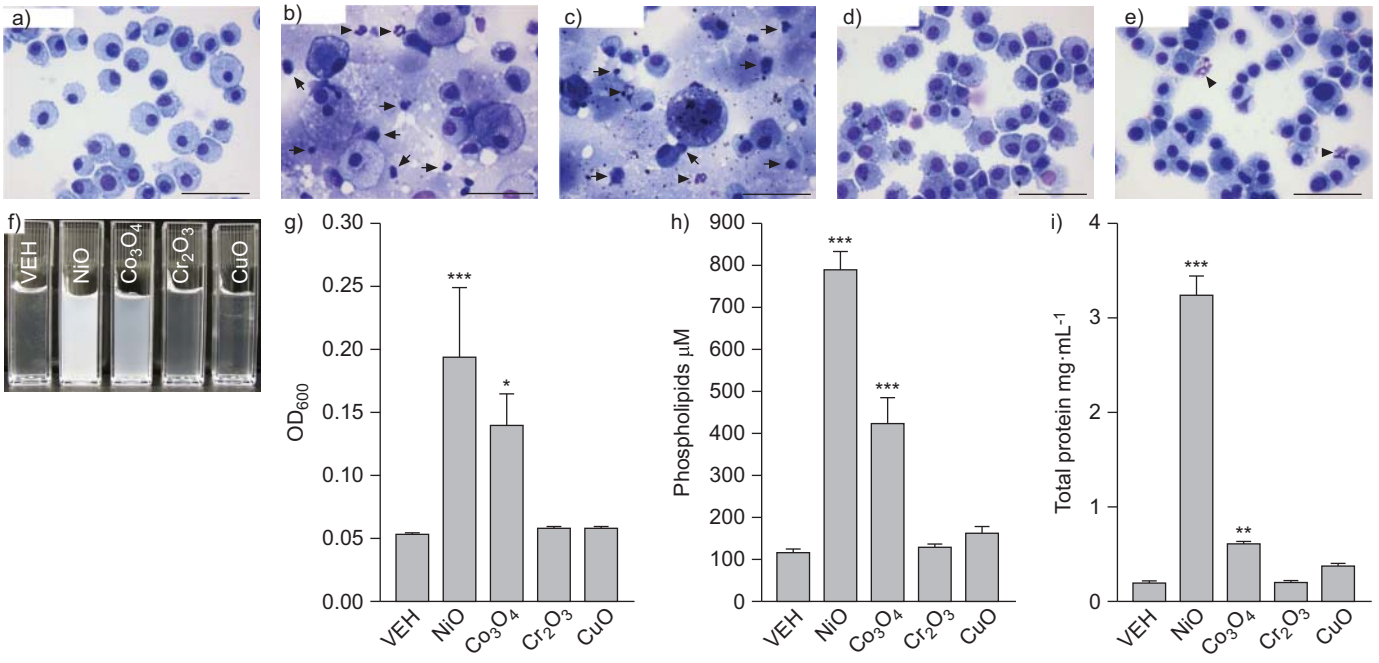

FIGURE 2. Bronchoalveolar lavage (BAL) analysis 4 weeks after instillation of NiO, Co_3O_4, Cr_2O_3 and CuO nanoparticles (NPs) at 150 cm^2. Representative images of BAL cells of a) vehicle (VEH) control, b) NiO NPs, c) Co_3O_4 NPs, d) Cr_2O_3 NPs and e) CuO NPs. Lymphocytes (arrow) were recruited by NiO and Co_3O_4 NPs, but not by Cr_2O_3 or CuO NPs. Neutrophil (arrowhead) infiltration was seen with NiO NPs, and occasionally in the Co_3O_4 and CuO NP treatment groups. Diff-Quik staining. Scale bars=50 μm. f) Representative colour of BAL fluid at 4 weeks after instillation of metal oxide NPs at 150 cm^2. Four samples per group were pooled in a quartz cuvette and pictures were taken with a digital camera. g) Turbidity was measured as optical density at 600 nm (OD_{600}). g) Turbidity, and levels of h) phospholipids and i) total proteins in the BAL were significantly increased by NiO and Co_3O_4 NP instillation. n=8 for all VEH and n=4 for other treatment groups. Each treatment group was compared with VEH for statistical significance. *: $p<0.05$; **: $p<0.01$; ***: $p<0.001$.

NPs were completely dissolved within 24 h, while other NPs showed slow and continuous dissolution.

Cytological analysis of BAL

Acute response

Figure 1 shows that, at 24 h after instillation, all NP-treated rats showed increased total cells (fig. 1a) in the BAL but with no changes in lymphocyte numbers (fig. 1d). The nature of the inflammation differed, however, as Cr_2O_3 NPs increased the numbers of macrophages (fig. 1b), whereas NiO, Co_3O_4 and CuO NPs increased granulocyte numbers (fig. 1c).

Chronic response

Figure 1 shows that 4 weeks after instillation, animals treated with CuO NPs had resolved the acute neutrophilia (fig. 1c) and were no different from the vehicle controls. Rats treated with NiO and Co_3O_4 NPs maintained the neutrophilia (fig. 1c) and, in addition, showed increased numbers of macrophages (fig. 1b) and lymphocytes (fig. 1d), indicating ongoing inflammation. The inflammation induced by Cr_2O_3 NP was similar to the acute response, with increased macrophages only, but without evidence of lymphocyte or granulocyte recruitment. Lymphocytes recruited into BAL by NiO NPs stained positively for both CD3 and CD45RA (online supplementary fig. S3).

Pulmonary alveolar proteinosis

Blue-staining proteinaceous material dominated the background of the cytospin slides of BAL cells from NiO and Co_3O_4 NP-treated rats at 4 weeks, and large foamy macrophages were also present (fig. 2b and c). The BAL fluid of NiO and Co_3O_4 NP-treated rats was milky and opaque, while those from Cr_2O_3 NP and CuO NP-treated animals were clear, similar to the vehicle control (fig. 2f). Consistent with the appearance, the measured turbidity, levels of phospholipids and total proteins in the BAL were also significantly increased in NiO and Co_3O_4 NP-treated, but not in Cr_2O_3 or CuO NP-treated, animals (fig. 2g–i).

Levels of autoantibodies for GM-CSF

As PAP can be associated with autoantibodies to GM-CSF, we tested BAL and serum samples 4 weeks after instillation, and no autoantibodies were detected (data not shown).

Effects of NPs on the ability of alveolar macrophages to catabolise DPPC

When added to alveolar macrophages, large amounts of NPs were phagocytosed within 2 h (fig. 3h–l), although CuO NPs could not be seen at the magnification used. When the culture medium was then removed, the cells washed and fresh medium supplemented with DPPC (250 μg·mL^{-1}) added, NiO and Co_3O_4 NP-treated alveolar macrophages became foamy, whilst Cr_2O_3 and CuO NPs maintained a normal macrophage appearance and size (fig. 3c–g). Without DPPC, foamy macrophages were not seen in any treatment groups. In concert with the development of a foamy appearance, the alveolar macrophages exposed to NiO and Co_3O_4 NPs were unable to clear DPPC from the medium (fig. 3a). Thus, the appearance of foamy macrophages indicated a build-up of DPPC within the macrophages, and was indicative of their failure to process and clear DPPC.

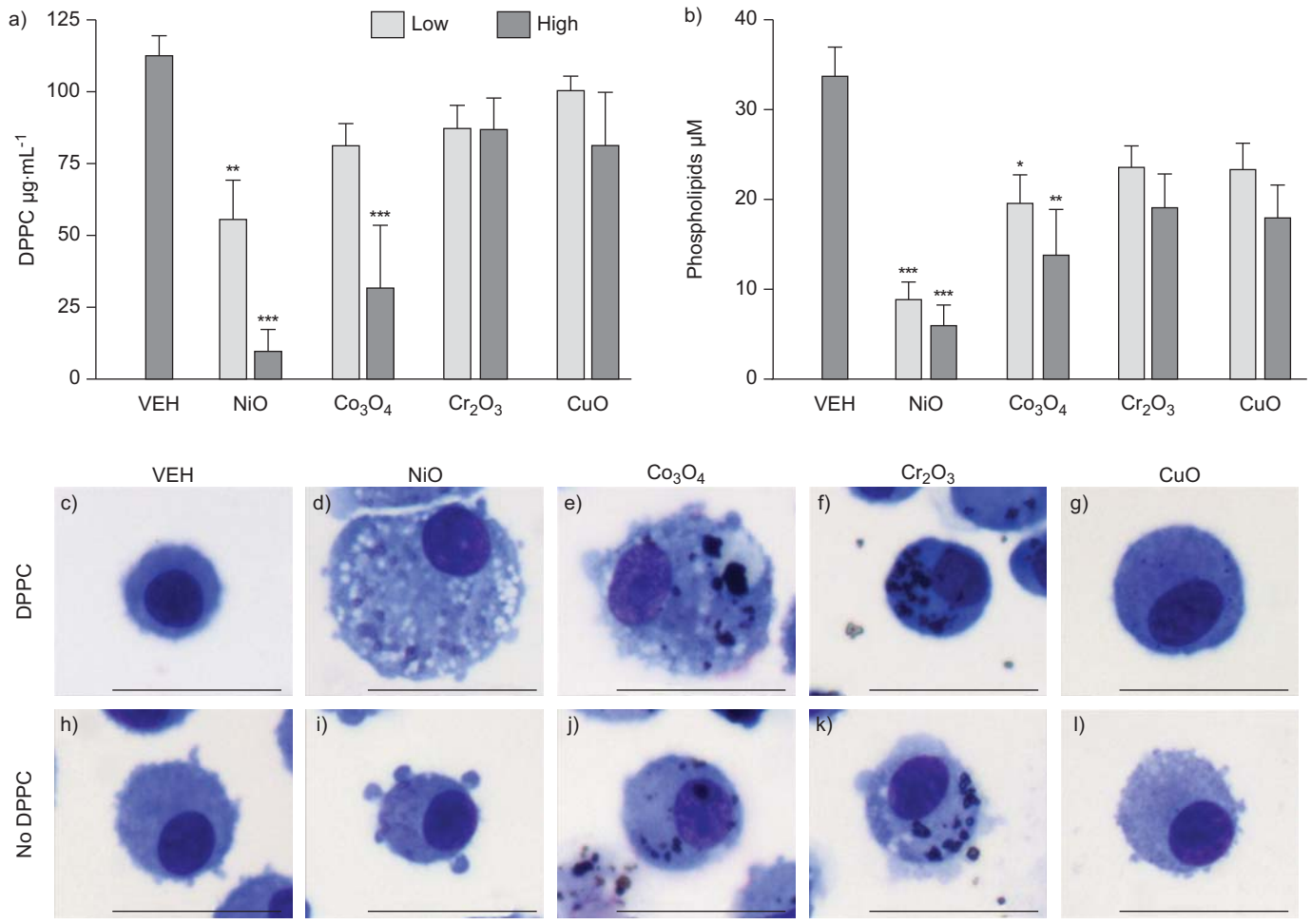

FIGURE 3. Clearance of dipalmitoylphosphatidylcholine (DPPC) by primary cultured alveolar macrophages (AMs). DPPC levels were measured by absorbance at 600 nm and quantified using a standard curve (r^2=0.999). NiO, Co_3O_4 and Cr_2O_3 nanoparticles (NPs) were added at 30 and 100 $cm^2 \cdot mL^{-1}$, while CuO NPs were added at 3 and 10 $cm^2 \cdot mL^{-1}$. NPs were treated for 2 h and cultured with or without DPPC (250 $\mu g \cdot mL^{-1}$). The levels of phospholipids in the DPPC and cell supernatant were measured using commercially available kits. The levels of cleared a) DPPC and b) phospholipids by AMs were significantly inhibited by NiO and Co_3O_4 NPs, while Cr_2O_3 and CuO NPs were comparable to vehicle (VEH) control. n=8 for all VEH and n=4 for other treatment groups. Data are presented as mean±SD. Each treatment group was compared with VEH for statistical significance. *: $p<0.05$; **: $p<0.01$; ***: $p<0.001$. c–l) Treatment of NiO and Co_3O_4 NP-treated groups with DPPC made AMs foamy, while Cr_2O_3 and CuO NPs did not. Without DPPC, no NPs induced foamy AMs. The representative cytospin images were taken from low-dose groups (3 $cm^2 \cdot mL^{-1}$ for CuO NPs and 30 $cm^2 \cdot mL^{-1}$ for others). Diff-Quik staining. Scale bars=25 μm.

There was a clear contrast between the substantial clearance of DPPC from the medium of the control, Cr_2O_3 NP-treated and CuO NP-treated alveolar macrophages, and the much reduced capacity for clearance shown by alveolar macrophages treated with the NiO and Co_3O_4 NPs (fig. 3a and b).

Histological analysis

Acute response

Consistent with the BAL data, at 24 h after instillation, NiO NPs induced moderate perivascular and peribronchiolar inflammation, and mild neutrophil infiltration in the alveoli (online supplementary fig. S4). Co_3O_4 NPs did not induce any interstitial inflammation but there was mild neutrophilia in the alveoli of rats treated with these NPs. Cr_2O_3 NP-treated rats showed no inflammation in any compartment. CuO NP-treated rats had moderate neutrophilic inflammation both in the interstitium and alveoli.

Chronic response

4 weeks after instillation, NiO and Co_3O_4 NP-exposed lungs showed foamy macrophages with proteinaceous deposits in the alveoli (fig. 4b and c) and large interstitial lymphoid aggregates (fig. 4f). The lymphocyte aggregates score was not variable between post-lavaged and nonlavaged lung (fig. 4f). The proteinaceous materials stained positively for glycoprotein with PAS staining (online supplementary fig. S5). Despite the increased numbers of macrophages seen in BAL, Cr_2O_3 NP-exposed lungs showed no inflammatory reaction in the interstitium (fig. 4d). CuO NP-treated rats showed mild-to-moderate granulomatous inflammation (fig. 4e).

Ki-67 immunohistochemistry

Figure 5 shows that lung tissues at 4 weeks after instillation of NiO and Co_3O_4 NPs showed a substantial population of cells with Ki-67-positive nuclei, which anatomically and morphologically

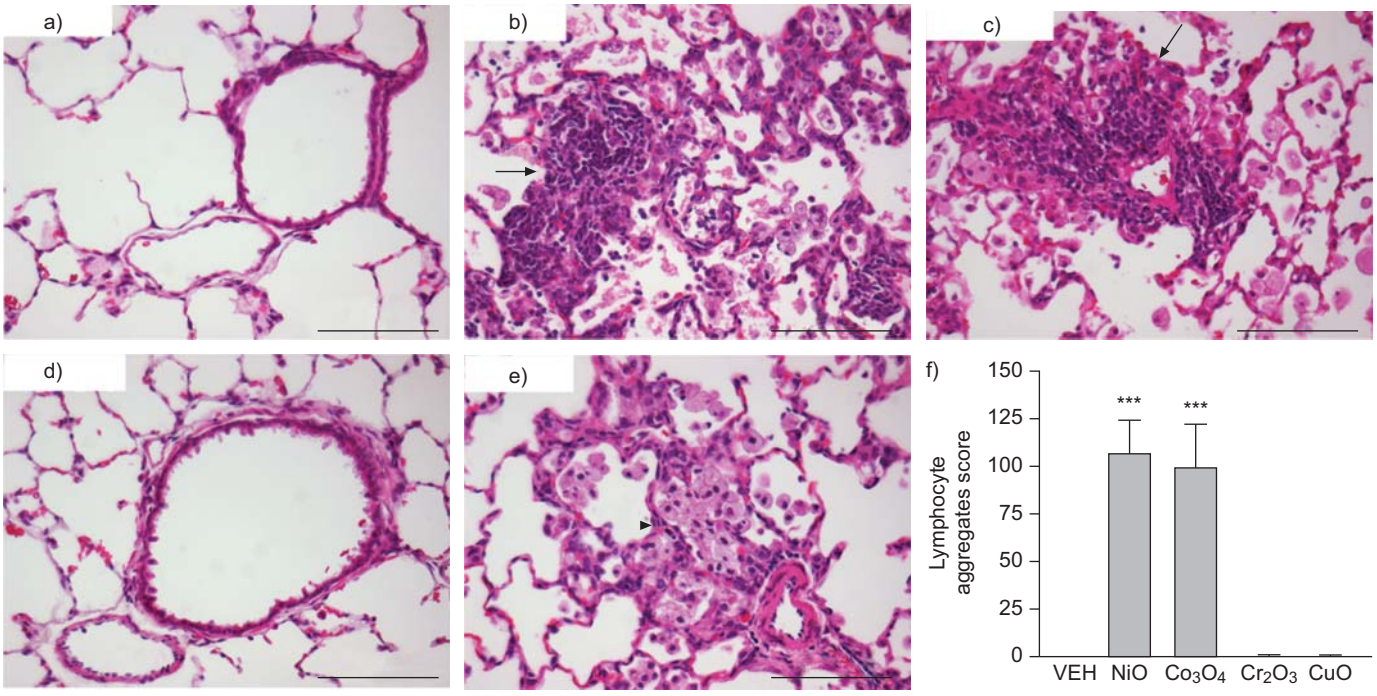

FIGURE 4. Lung histology 4 weeks after instillation of metal oxide nanoparticles (NPs) to rats at 150 cm^2. Representative lung histology of a) vehicle (VEH) control, b) NiO NPs, c) Co_3O_4 NPs, d) Cr_2O_3 NPs and e) CuO NPs. NiO and Co_3O_4 NP produced lymphocyte aggregates (arrow), foamy macrophages and deposition of proteinaceous material in the alveoli. Cr_2O_3 NPs did not cause any inflammatory reactions, while CuO NPs induced chronic granulomatous inflammation (arrowhead). Tissues were stained with haematoxylin and eosin. Scale bars=100 μm. f) Lymphocyte aggregates score was determined by counting the number of lymphocyte aggregates in the alveoli, excluding peribronchial lymph nodes, in each lobe and multiplying by a factor representing the diameter of aggregates as follows: 1, <50 μm; 2, 50–200 μm; or 3, >200 μm. Data are presented as mean±SD. Each treatment group was compared with VEH for statistical significance. ***: $p<0.001$.

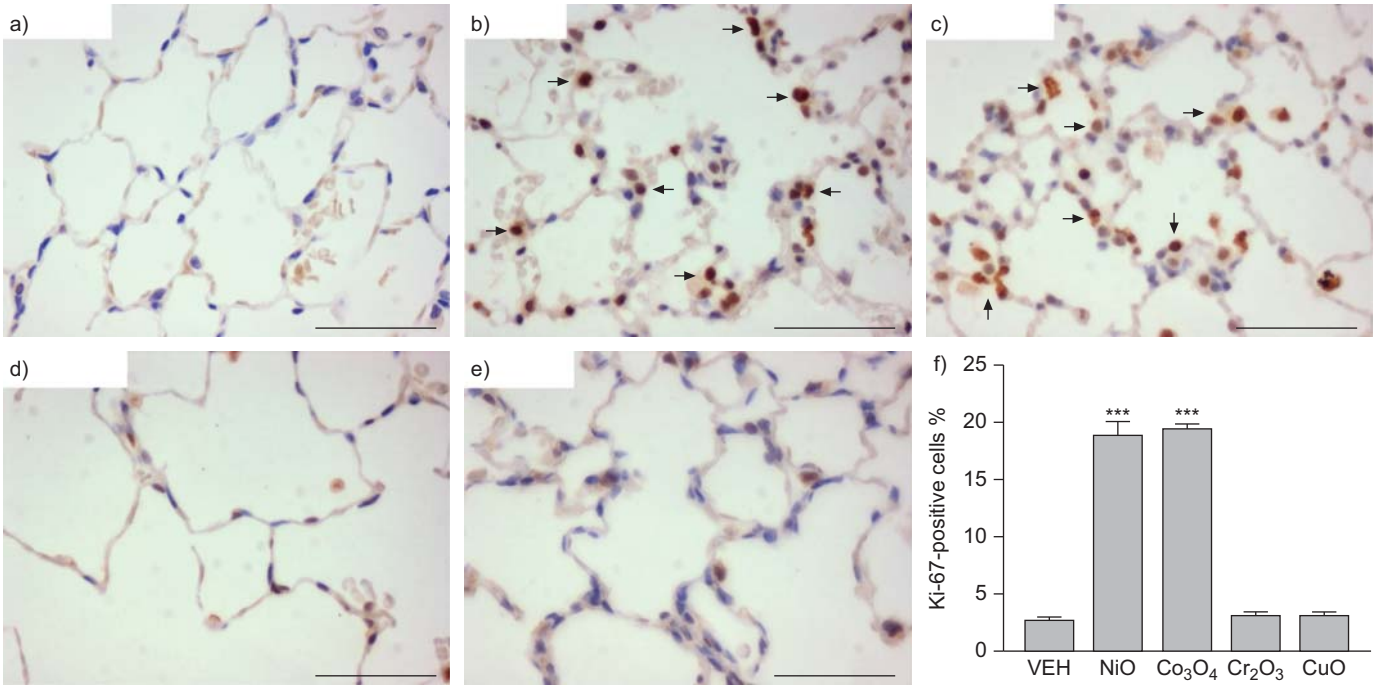

FIGURE 5. Immunohistochemistry for Ki-67 in the lungs 4 weeks after instillation of metal oxide nanoparticles (NPs) at 150 cm^2. Ki-67-positive cells were found in the alveolar type II-like cells (arrow) in the b) NiO and c) Co_3O_4 NP-treated lungs. a) Vehicle (VEH) control, d) Cr_2O_3 NPs and e) CuO NPs showed no positive signals in the alveolar epithelium. Each panel is a representative section of the lungs from the various exposed groups. Scale bars=50 μm. f) Percentages of Ki-67-positive nuclei in the alveolar region, excluding blood vessels and bronchioles, were determined on four slides for each group and expressed as mean±SD. n=8 for all VEH and n=4 for other treatment groups. Each treatment group was compared with VEH for statistical significance. ***: $p<0.001$.

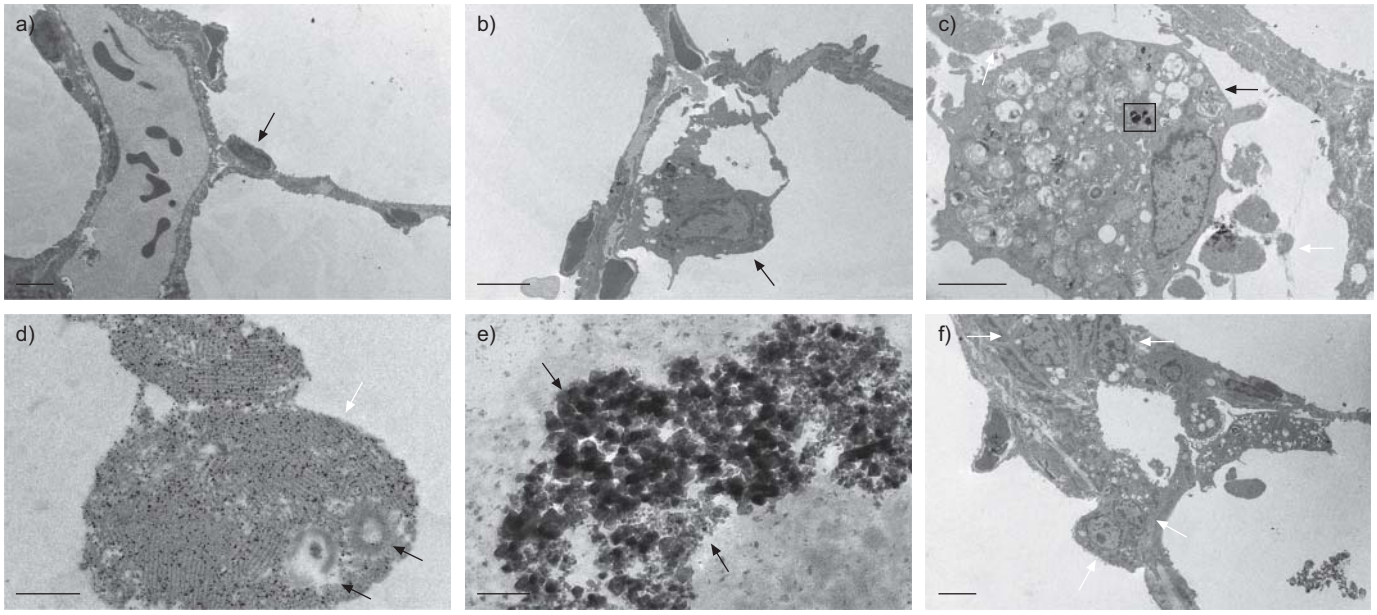

FIGURE 6. Representative images of a, b) vehicle control and c–f) NiO nanoparticles (NPs) 4 weeks post-instillation. a) Normal alveolar structure consisting of thin type I cells (black arrow). b) Compared with small macrophages in the vehicle control (black arrow), c) large foamy macrophages were found in the alveoli of NiO NP-treated lungs (black arrow); note that foamy macrophages contained numerous complex phospholipoprotein inclusions. c) Proteinaceous material was deposited in the alveoli (white arrow), and d) a higher-power view revealed these to be consistent with the large-aggregate form of surfactant (white arrow) and lamellar bodies (black arrows). e) Higher-power view of the electron-dense granules located in the rectangle inside the foamy macrophage in c), revealing them to be NiO NPs (black arrows). f) Low-power view to show proliferating and vacuolated type II epithelial cells in NiO NP-treated lungs (white arrows). Scale bars: a) 5 μm; b) 5 μm; c) 2 μm; d) 0.5 μm; e) 0.1 μm; f) 5 μm.

appeared to be type II alveolar epithelial cells. We identified type II cells as proliferating cells that were Ki-67 positive and positioned in the septa wall; it is well established that the only proliferating cell in the alveolar wall during lung injury is the type II alveolar epithelial cell [18]. Lungs from rats exposed to the vehicle control, Cr_2O_3 NPs and CuO NPs showed very few Ki-67-positive nuclei in the alveolar region (fig. 5d and e). The percentage of Ki-67-positive cells in the alveolar walls in NiO and Co_3O_4 NP-treated lungs was ~20%, while vehicle control, Cr_2O_3 NPs and CuO NPs showed ~3% positivity (fig. 5f).

TEM analysis of NiO NP-exposed lungs

Control lungs showed normal alveolar septa, capillaries, type II cells and occasional alveolar macrophages in the alveolar lumen (fig. 6a and b). In contrast, numerous foamy macrophages and profuse lipoproteinaceous material were found in the alveolar spaces in NiO NP-treated lungs 4 weeks after instillation (fig. 6c and d). The foamy macrophages contained numerous vesicles and lamellar bodies, which are known to contain surfactant proteins and phospholipids. In addition, NiO NPs were visible inside the foamy macrophages (fig. 6e). Alveolar type II cells were increased in number and contained numerous vacuoles, compared with those of the vehicle control (fig. 6f). The proteinaceous materials in the alveoli were consistent with surfactant in the form of large aggregates and lamellar bodies.

Cytokines in the BAL

In order to evaluate the mediators that might account for the observed inflammatory responses, we analysed BAL and serum for the chemokines MCP-1/CCL2 (chemotactic for monocytes, granulocytes and lymphocytes), MIP-2/CXCL2 (chemotactic for granulocytes and lymphocytes), IL-12 p40 (induces Th1 effector cells), the pro-inflammatory Th1-associated cytokine IFN-γ, the Th2-associated cytokine IL-4, the Th17 effector cell-associated cytokine IL-17A and GM-CSF (induced by inflammation and by lung exposure to NPs).

In the serum samples from NP-exposed rats, there were no significant changes in any cytokines compared with vehicle control at either time-point, whereas in BAL, the different NP treatments induced different patterns of cytokine/chemokine release, indicating that the inflammatory responses generated were compartmentalised in the lungs.

Figure 7 shows that levels of MCP-1/CCL2 were significantly increased by NiO and Co_3O_4 NPs in both the acute and chronic phases, while CuO NPs induced MCP-1/CCL2 only in the acute phase. The levels of MIP-2/CXCL2 were significantly increased by NiO, Co_3O_4 and CuO NPs 24 h post-instillation, and had returned to control levels by 4 weeks. The levels of IL-12 p40 were significantly increased by CuO NPs at 24 h, and by NiO and Co_3O_4 NPs 4 weeks after instillation. IFN-γ levels were significantly elevated compared with the vehicle control only by NiO NPs at 4 weeks. IL-17A was significantly increased at 24 h by CuO NPs and at 4 weeks by NiO NP instillation, compared with the vehicle control. GM-CSF and IL-4 showed no significant changes in any treatment group compared with controls.

The effects of serum coating on the toxicity of NiO NPs

Both serum-coated NiO NPs and NiO NPs without coronas (*i.e.* uncoated) produced DTH-like inflammation and PAP (online supplementary figs. S6 and S7). However, uncoated NiO NPs showed significantly less potential for producing DTH-like inflammation (number of lymphocytes) and PAP (levels of phospholipids and total protein) compared with serum-coated NiO NPs.

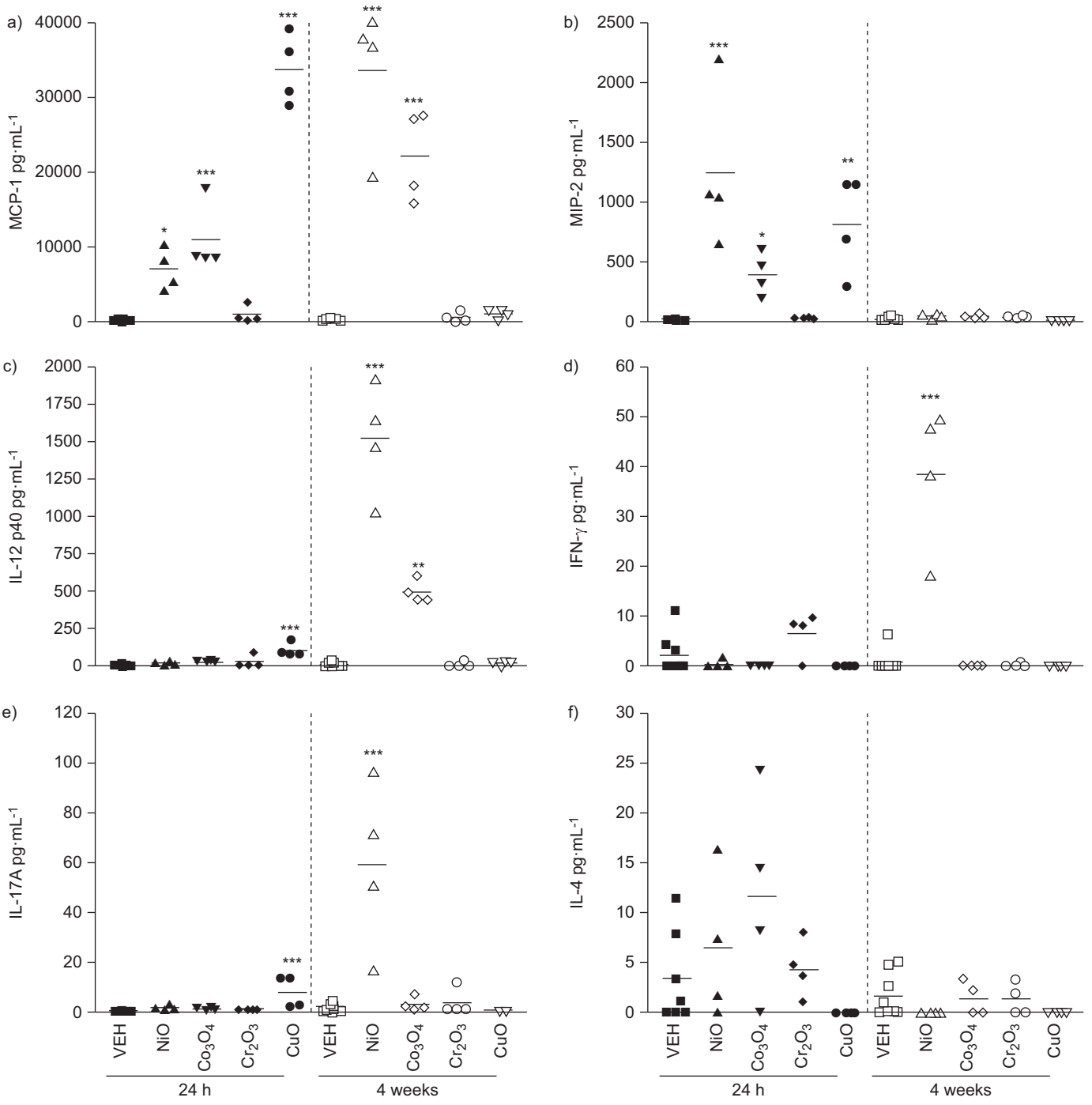

FIGURE 7. Concentrations of a) monocyte chemotactic protein (MCP)-1/CCL2, b) macrophage inflammatory protein (MIP)-2/CXCL2, c) interleukin (IL)-12 p40, d) IL-17A, e) interferon (IFN)-γ and f) IL-4 in bronchoalveolar lavage after instillation of metal oxide nanoparticles at 150 cm^2. n=8 for all vehicle control and n=4 for other treatment groups. —: mean. Each treatment group was compared with vehicle (VEH) control for statistical significance. *: $p<0.05$; **: $p<0.01$; ***: $p<0.001$.

DISCUSSION

In our previous work, we found that metal oxide NPs release water-soluble ions and that instillation of these into rat lungs induced contrasting types and kinetics of inflammation [1, 12]. Some metal ions, including Ni(II), Co(II, III), Cr(III) and Cu(II), have been reported to induce DTH (characterised by Th1 and/or Th17 effector cell activation) in human skin *via* haptenisation of proteins [8]. Since such metal ions induce allergic responses in skin and metal oxide NPs release metal ions, we hypothesised that NPs comprised of the oxides of haptenic metals might induce DTH-like inflammation and pathology in the lungs.

The pathological appearance of lungs at 4 weeks largely agreed with the BAL cellular profile. Cr_2O_3 NPs produced no inflammatory effects acutely or chronically, while CuO NPs

caused a transient, acute inflammation in the BAL that had resolved, leaving a modest granulomatous inflammation evident in histological sections by 4 weeks. In contrast, both NiO and Co_3O_4 NPs produced acute neutrophilic inflammation and caused worsening DTH-like mononuclear inflammation, characterised by PAP, epithelial proliferation, lymphocytic foci and granulocytic infiltration of the airspace. NiO NPs have been known to cause acute neutrophilic inflammation [1, 12], and chronic inflammation consisting of lymphocytes and neutrophils [12, 19]. Co_3O_4 NPs, without dispersion media, did not significantly increase the polymorphonuclear neutrophil number when instilled at surface area dose of 250 cm^2 per rat, although increased reactive oxygen species were detectable, which might trigger acute neutrophilic inflammation [1]. This discrepancy with our data might be due to the improved dispersion of our NPs; well-dispersed NPs show much higher inflammatory potential compared with poorly dispersed NPs [20]. CuO NPs cause acute neutrophilic inflammation and chronic granulomatous inflammation when instilled into lungs of rats [12, 21]. However, the chronic effects of Co_3O_4 and Cr_2O_3 NPs, and the immunological effects of our panel of NPs have not been previously reported.

Allogeneic rat serum acts as an excellent dispersant for NPs without risks of ''foreign-ness''. When NPs are inhaled, they deposit on the surfactant lipoprotein surface lining of the lung. This surfactant lipoprotein immediately forms a corona on the surface of the NPs. Both serum-coated and uncoated NiO NPs showed significant DTH-like inflammation and PAP compared with the vehicle control. However, the potential for provoking these pathologies by serum-coated NiO NPs were significantly greater than that of uncoated NiO NPs. This difference is most probably due to the improved dispersion rather than serum protein-specific effects of serum-coated NiO NPs.

All NPs showed minimal solubility in physiological saline and basic artificial interstitial fluid (pH 7.4), which mimics pulmonary interstitial fluid [15], while NPs showed a heterogeneous range of solubilities under acidic conditions (pH 5.5), which mimic the lysosomal environment of alveolar macrophages [14, 22]. In this acid environment, CuO NPs were completely dissolved within 24 h, while other NPs showed a slow and continuous dissolution pattern in the order $NiO>Co_3O_4>Cr_2O_3$. Therefore, because of fast dissolution and clearance, CuO NPs might have no opportunity to be haptenic [23]. However, NiO and Co_3O_4 NPs showed slow continuous dissolution, providing a ''slow release'' of challenging hapten over 4 weeks, eventually provoking DTH-like inflammation. Cr_2O_3 NPs showed the least and minimal dissolution among our panel of NPs, and this might not be sufficient to be haptenic. This dissolution is consistent with the findings of many particles in alveolar macrophages treated with NiO, Co_3O_4 and Cr_2O_3 NPs, while no CuO NPs could be seen 4 weeks after instillation. The kinetics of micron-sized nickel compounds showed that the half-life of an inhaled soluble form of a nickel compound ($NiSO_4$) was 2–3 days in rats and <1 day in mice [24], while an insoluble form of a nickel compound (NiO; 2–2.4 μm) was 33 [24] or 120 days [25] in rats. The half-life of inhaled nanosized NiO (139 ± 12 nm) was 62 days in rats [26]. In this study, we have not challenged putative antigen at a distal site, since this was not the aim of the study; therefore, we have not demonstrated classical DTH. However, we contend that the ongoing release of soluble ions from biopersistent NPs resident in the lungs provides ongoing challenge, producing a DTH-like response. Neither the primary particle size nor hydrodynamic size showed any relationship with the DTH potential.

The mass doses of the panel of NPs used here (163.5–515.0 μg) can be contextualised to plausible lung doses. For example, a predicted alveolar retained mass of 163.5 μg would result from 10 days of exposure to a 650 $\mu g \cdot m^{-3}$ cloud of NPs with aerodynamic diameter of 100 nm (consistent with the hydrodynamic sizes in this study) according to the multiple-path particle dosimetry deposition model [27]. According to the US Environmental Protection Agency, the American Conference of Governmental and Industrial Hygienists' threshold limit value of insoluble nickel and metal compounds is 200 and 1,500 $\mu g \cdot m^{-3}$, respectively [28].

The cellular inflammatory responses we measured in the lungs had a biologically plausible relationship with the cytokines/chemokines measured in the BAL. Initially CD3-positive T-cells were a feature of the BAL infiltrate in NiO and Co_3O_4 NP-instilled lungs. None of the NPs tested induced IL-4 secretion, indicating a lack of any Th2-related immunity. MCP-1/CCL2 plays an important role in recruiting monocytes/macrophages [29], neutrophils [30] and T-cells [31], and MIP-2/CXCL2 recruits neutrophils [32]. Therefore, the increased levels of MCP-1/CCL2 and MIP-2/CXCL2 induced by NiO, Co_3O_4 and CuO NPs during the acute phase were consistent with the increased number of granulocytes in BAL. The increases in MCP-1/CCL2 induced by NiO and Co_3O_4 NPs during the chronic phase were also consistent with the increased number and type of BAL cells. MCP-1/CCL2 might mediate DTH by stimulating Th1-related cytokine expression [29]. IL-12 promotes Th1 responses and stimulates IFN-γ production [33]. IL-17A is associated with Th17 effector cells and neutrophil recruitment, and also stimulates Th1 immunity [34]. NiO and Co_3O_4 NPs induced a sustained increase in lymphocyte and macrophage cell numbers in BAL and interstitial lymphocytic aggregates. However, NiO and Co_3O_4 NPs had a different cytokine induction profile, with NiO NPs inducing secretion of both Th1-associated (IL-12 p40 and IFN-γ) and Th17-associated (IL-17A) cytokines in BAL at the later time-point, whereas Co_3O_4 NP-instilled animals only had measurable IL-12 p40, indicating less Th1 and no sustained Th17 activation. In contrast, despite releasing metal ions known to cause skin DTH [8], Cr_2O_3 and CuO NPs showed no lymphocytic response in BAL or the lung interstitium, and no sustained Th1- or Th17-related cytokine response. There is overwhelming evidence in the literature that the four metals used in NP oxide form in this study are haptenic in the skin as metal ions [8]. We show here that, in oxide nanoparticulate form, the same metals are heterogeneous in terms of their ability to induce pulmonary DTH-like responses in rats. NiO and Co_3O_4 NPs stood out in contrast to the other two metal oxide NPs as causing sustained lymphocytic infiltrate into the BAL, lymphocyte aggregates in lung section and increases in both MCP1/CCL2 and IL-12 p40 in the BAL. In addition, NiO NPs caused increases in IFN-γ and IL-17A. Thus, classical markers of Th1/DTH responses are increased, albeit with the NiO NPs appearing to be more potent than Co_3O_4 NPs in this regard.

The PAP induced by NiO and Co_3O_4 NPs in rats has similar features to human and primate alveolar lipoproteinosis [35].

The surfactant lipoprotein forming the epithelial lining fluid is normally in dynamic equilibrium through the actions of the alveolar type II cells, which synthesise and secrete it, and alveolar macrophages and alveolar type II cells, which clear and recycle it [11]. PAP is either genetic, or secondary to haematological malignancies, autoimmune diseases or particle inhalation, and can be associated with production of anti-GM-CSF autoantibodies [10]. Particles can produce PAP by dust overload or with a toxic dust at lower dose. Particles known to induce secondary alveolar proteinosis include silica, titanium, indium tin oxide, aluminium and cement [10]. However, the pathogenesis of PAP induced by particle inhalation is poorly understood. Deposition of particles in the lung induces alveolar type II cell proliferation and/or impairs the function of surfactant clearance by killing alveolar macrophages [36]. However, a recent study with indium tin oxide [37] and a large cohort study from Japan [38] both showed that particle or dust exposure might be linked with autoimmune alveolar proteinosis by inducing autoantibodies to GM-CSF. We found no evidence of anti-GM-CSF autoantibodies in any of the animals with PAP. Therefore, at least in our experiments, PAP induced by NiO and Co_3O_4 NPs was not associated with autoantibodies against GM-CSF. In the present study, we found that NiO and Co_3O_4 NPs induced PAP. *In vitro*, these NPs impaired the clearance of DPPC by primary alveolar macrophages and induced foamy macrophage morphology, mimicking events in the lungs. In contrast, Cr_2O_3 and CuO NPs did not cause foamy macrophage formation and did not affect DPPC clearance by macrophages *in vitro*, although the NPs were fully engulfed. NiO and Co_3O_4 NP-treated rats also demonstrated increased proliferation of alveolar type II cells, which are responsible for surfactant production. Thus, the overproduction of surfactant by proliferation of alveolar type II cells and the impairment of macrophage surfactant clearance probably combined to induce the PAP in NP-exposed lungs.

In the present study, we only focused on a small subset of metal oxide NPs and their long-term immunological effects following a single instillation. We do not suggest that these effects are nano-specific and, in fact, many kinds of micron-sized particles cause immunological effects (*e.g.* beryllium). It is important to discover the mechanisms of NP effects, whatever they may be, since NP exposures are set to increase as NPs are utilised more in industrial processes, necessitating hazard identification to aid the risk assessment process. In addition, we do not consider that the mechanism shown here for the two immunologically active NPs is generic for all NPs. Different NPs cause their effects by different mechanisms dependent on their composition and shape, and we focused here only on one small subset of NP type and one type of immunopathological response. Nanosized particles have been known to cause more severe pulmonary toxicity than micron-sized particles [19], and the immunopathological responses that are elicited might be much greater than those of micron-sized particles as a result of greater retention and increased solubility from their greater surface area. This is also supported by the increased DTH potential of well-dispersed NiO NPs (92 nm hydrodynamic size) than highly aggregated NiO NPs (6 μm hydrodynamic size). The National Toxicology Program in the USA performed a 2-yr inhalation study using nickel compounds and showed that micron-sized nickel compounds, including an insoluble form (NiO; 2.2 ± 2.6 mm) and soluble forms ($NiSO_4$ and Ni_3S_2), caused alveolar proteinosis in the lung and lymphoid hyperplasia in the bronchial lymph nodes [39–41]. Because the NPs studied here are being manufactured for diverse purposes, including use as catalysts, semiconductors and pigments [42], accidental occupational exposure is likely. Our data suggest that a single accidental exposure to certain haptenic metal oxide NPs might produce prolonged and worsening immunopathological responses.

In conclusion, NPs comprised of oxides of metals known to be haptenic in skin had variable potential to induce DTH-like responses and PAP in the lungs of rats after a single instillation exposure. While NiO and Co_3O_4 NP exposures were associated with a worsening immunoinflammatory response, producing PAP and immunologically mediated lung damage, Cr_2O_3 and CuO NPs were not active in this regard. This has important implications for risk management of some NPs, indicating that a single elevated exposure to some NPs in an occupational setting might trigger a progressive lung disease characteristic of DTH. This may be a result of the slow release of metal ions from NPs causing repeated cycles of haptenisation of host proteins, leading to chronic autoimmune inflammation.

SUPPORT STATEMENT

Financial support for this study was provided by the Medical Research Council (London, UK; grant MRC G0701323).

STATEMENT OF INTEREST

A statement of interest for W. MacNee can be found at www.erj.ersjournals.com/site/misc/statements.xhtml

REFERENCES

1 Lu S, Duffin R, Poland C, *et al.* Efficacy of simple short-term *in vitro* assays for predicting the potential of metal oxide nanoparticles to cause pulmonary inflammation. *Environ Health Perspect* 2009; 117: 241–247.
2 McNeilly JD, Heal MR, Beverland IJ, *et al.* Soluble transition metals cause the pro-inflammatory effects of welding fumes *in vitro*. *Toxicol Appl Pharmacol* 2004; 196: 95–107.
3 Kobayashi K, Kaneda K, Kasama T. Immunopathogenesis of delayed-type hypersensitivity. *Microsc Res Tech* 2001; 53: 241–245.
4 Rajesh D, Zhou Y, Jankowska-Gan E, *et al.* Th1 and Th17 immunocompetence in humanized NOD/SCID/IL2rγ^{null} mice. *Hum Immunol* 2010; 71: 551–559.
5 Sakai M, Yamashita K, Takemoto N, *et al.* Diesel exhaust (DE) aggravates pathology of delayed-type hypersensitivity (DTH) induced by methyl-bovine serum albumin (mBSA) in mice. *J Toxicol Sci* 2009; 34: 483–492.
6 Thierse HJ, Gamerdinger K, Junkes C, *et al.* T cell receptor (TCR) interaction with haptens: metal ions as non-classical haptens. *Toxicology* 2005; 209: 101–107.
7 Martin SF. T lymphocyte-mediated immune responses to chemical haptens and metal ions: implications for allergic and autoimmune disease. *Int Arch Allergy Immunol* 2004; 134: 186–198.
8 Budinger L, Hertl M. Immunologic mechanisms in hypersensitivity reactions to metal ions: an overview. *Allergy* 2000; 55: 108–115.
9 Imanishi T, Hasegawa M, Sudo A. Serum metal ion levels after second-generation metal-on-metal total hip arthroplasty. *Arch Orthop Trauma Surg* 2010; 130: 1447–1450.
10 Costabel U, Nakata K. Pulmonary alveolar proteinosis associated with dust inhalation: not secondary but autoimmune? *Am J Respir Crit Care Med* 2010; 181: 427–428.

11 Shah PL, Hansell D, Lawson PR, *et al.* Pulmonary alveolar proteinosis: clinical aspects and current concepts on pathogenesis. *Thorax* 2000; 55: 67–77.
12 Cho WS, Duffin R, Poland CA, *et al.* Metal oxide nanoparticles induce unique inflammatory footprints in the lung; important implications for nanoparticle testing. *Environ Health Perspect* 2010; 118: 1699–1706.
13 Trapnell BC, Carey BC, Uchida K, *et al.* Pulmonary alveolar proteinosis, a primary immunodeficiency of impaired GM-CSF stimulation of macrophages. *Curr Opin Immunol* 2009; 21: 514–521.
14 Stopford W, Turner J, Cappellini D, *et al.* Bioaccessibility testing of cobalt compounds. *J Environ Monit* 2003; 5: 675–680.
15 Moss OR. Simulants of lung interstitial fluid. *Health Phys* 1979; 36: 447–448.
16 Trapnell BC, Whitsett JA. GM-CSF regulates pulmonary surfactant homeostasis and alveolar macrophage-mediated innate host defense. *Annu Rev Physiol* 2002; 64: 775–802.
17 Tonks A, Parton J, Tonks AJ, *et al.* Surfactant phospholipid DPPC downregulates monocyte respiratory burst *via* modulation of PKC. *Am J Physiol Lung Cell Mol Physiol* 2005; 288: L1070–L1080.
18 Yee M, Vitiello PF, Roper JM, *et al.* Type II epithelial cells are critical target for hyperoxia-mediated impairment of postnatal lung development. *Am J Physiol Lung Cell Mol Physiol* 2006; 291: L1101–L1111.
19 Ogami A, Morimoto Y, Myojo T, *et al.* Pathological features of different sizes of nickel oxide following intratracheal instillation in rats. *Inhal Toxicol* 2009; 21: 812–818.
20 Duffin R, Tran L, Brown D, *et al.* Proinflammogenic effects of low-toxicity and metal nanoparticles *in vivo* and *in vitro*: highlighting the role of particle surface area and surface reactivity. *Inhal Toxicol* 2007; 19: 849–856.
21 Yokohira M, Kuno T, Yamakawa K, *et al.* Lung toxicity of 16 fine particles on intratracheal instillation in a bioassay model using f344 male rats. *Toxicol Pathol* 2008; 36: 620–631.
22 Nyberg K, Johansson U, Johansson A, *et al.* Phagolysosomal pH in alveolar macrophages. *Environ Health Perspect* 1992; 97: 149–152.
23 Hirano S, Ebihara H, Sakai S, *et al.* Pulmonary clearance and toxicity of intratracheally instilled cupric oxide in rats. *Arch Toxicol* 1993; 67: 312–317.
24 Benson JM, Chang IY, Cheng YS, *et al.* Particle clearance and histopathology in lungs of F344/N rats and B6C3F1 mice inhaling nickel oxide or nickel sulfate. *Fundam Appl Toxicol* 1995; 28: 232–244.
25 Benson JM, Barr EB, Bechtold WE, *et al.* Fate of inhaled nickel oxide and nickel subsulfide in F344/N rats. *Inhal Toxicol* 1994; 6: 167–183.
26 Oyabu T, Ogami A, Morimoto Y, *et al.* Biopersistence of inhaled nickel oxide nanoparticles in rat lung. *Inhal Toxicol* 2007; 19: Suppl. 1, 55–58.
27 Cassee FR, Muijser H, Duistermaat E, *et al.* Particle size-dependent total mass deposition in lungs determines inhalation toxicity of cadmium chloride aerosols in rats. Application of a multiple path dosimetry model. *Arch Toxicol* 2002; 76: 277–286.
28 Environmental Protection Agency. Nickel Compounds. www.epa.gov/ttn/atw/hlthef/nickel.html Date last updated: November 2007. Date last accessed: January 2012.
29 Boring L, Gosling J, Chensue SW, *et al.* Impaired monocyte migration and reduced type 1 (Th1) cytokine responses in C-C chemokine receptor 2 knockout mice. *J Clin Invest* 1997; 100: 2552–2561.
30 Maus U, von Grote K, Kuziel WA, *et al.* The role of CC chemokine receptor 2 in alveolar monocyte and neutrophil immigration in intact mice. *Am J Respir Crit Care Med* 2002; 166: 268–273.
31 Carr MW, Roth SJ, Luther E, *et al.* Monocyte chemoattractant protein 1 acts as a T-lymphocyte chemoattractant. *Proc Natl Acad Sci USA* 1994; 91: 3652–3656.
32 Fitch PM, Wheelhouse NM, Bowles P, *et al.* Ectopic lymphoid tissue formation in the lungs of mice infected with *Chlamydia pneumoniae* is associated with epithelial macrophage inflammatory protein-2/CXCL2 expression. *Clin Exp Immunol* 2010; 162: 372–378.
33 Meyts I, Hellings PW, Hens G, *et al.* IL-12 contributes to allergen-induced airway inflammation in experimental asthma. *J Immunol* 2006; 177: 6460–6470.
34 Bai H, Cheng J, Gao X, *et al.* IL-17/Th17 promotes type 1 T cell immunity against pulmonary intracellular bacterial infection through modulating dendritic cell function. *J Immunol* 2009; 183: 5886–5895.
35 Sakagami T, Beck D, Uchida K, *et al.* Patient-derived granulocyte/macrophage colony-stimulating factor autoantibodies reproduce pulmonary alveolar proteinosis in nonhuman primates. *Am J Respir Crit Care Med* 2010; 182: 49–61.
36 Corrin B, King E. Pathogenesis of experimental pulmonary alveolar proteinosis. *Thorax* 1970; 25: 230–236.
37 Cummings KJ, Donat WE, Ettensohn DB, *et al.* Pulmonary alveolar proteinosis in workers at an indium processing facility. *Am J Respir Crit Care Med* 2010; 181: 458–464.
38 Inoue Y, Trapnell BC, Tazawa R, *et al.* Characteristics of a large cohort of patients with autoimmune pulmonary alveolar proteinosis in Japan. *Am J Respir Crit Care Med* 2008; 177: 752–762.
39 National Toxicology Program. NTP toxicology and carcinogenesis studies of nickel oxide (CAS No. 1313-99-1) in F344 rats and B6C3F1 mice (inhalation studies). *Natl Toxicol Program Tech Rep Ser* 1996; 451: 1–381.
40 National Toxicology Program. NTP toxicology and carcinogenesis studies of nickel subsulfide (CAS No. 12035-72-2) in F344 rats and B6C3F1 mice (inhalation studies). *Natl Toxicol Program Tech Rep Ser* 1996; 453: 1–365.
41 National Toxicology Program. NTP toxicology and carcinogenesis studies of nickel sulfate hexahydrate (CAS No. 10101-97-0) in F344 rats and B6C3F1 mice (inhalation studies). *Natl Toxicol Program Tech Rep Ser* 1996; 454: 1–380.
42 Borm PJ, Robbins D, Haubold S, *et al.* The potential risks of nanomaterials: a review carried out for ECETOC. *Part Fibre Toxicol* 2006; 3: 11.